Supporting Information: Accuracy and Resource Estimations for Quantum Chemistry on a Near-term Quantum Computer

Michael Kühn[a*], Sebastian Zanker[b], Peter Deglmann[a], Michael Marthaler[b#], Horst Weiß[a]

[a]BASF SE – Quantum Chemistry Materials
Carl-Bosch-Str. 38, 67063 Ludwigshafen, Germany

[b]HQS Quantum Simulations
Haid-und-Neu-Str. 18, 76131 Karlsruhe, Germany

[*]e-mail: michael.b.kuehn@basf.com, [#]e-mail: michael.marthaler@quantumsimulations.de

(Dated: July 9, 2019)

Table I. Accuracy of molecular energies obtained with UCCSD-VQE for LiH, Li, NH_3, H_2 and CH_2. The HF total energy as well as the CCSD, CCSD(T), FCI and UCCSD-VQE correlation energies are given together with the respective differences to the FCI energy (ΔFCI). Additionally, the number of required qubits and two-qubit gates is shown. All results were obtained using the minimal basis set STO-3G. Energies are in kJ/mol.

	LiH		**Li**		**NH_3**		**H_2**		**CH_2**	
		ΔFCI		ΔFCI		ΔFCI		ΔFCI		ΔFCI
E_{total}(HF)	-20642.0	–	-19206.9	–	-145594.2	–	-2931.8	–	-100745.6	–
E_{corr}(CCSD)	-53.320	0.028	-0.815	0.000	-169.299	0.567	-54.085	0.000	-157.212	1.206
E_{corr}(CCSD(T))	-53.342	0.006	-0.815	0.000	-169.618	0.248	-54.085	0.000	-157.759	0.658
E_{corr}(FCI)	-53.348	0	-0.815	0	-169.866	0	-54.085	0	-158.417	0
E_{corr}(UCCSD-VQE)	-53.320	0.028	-0.815	0.000	-169.400	0.466	-54.085	0.000	-157.491	0.927
# qubits	12	–	10	–	14	–	4	–	12	–
# two-qubit gates	1382	–	464	–	5976	–	56	–	1366	–

Table II. Accuracy of LiH molecular energies obtained with UCCSD-VQE for basis sets of increasing size (SV, DZ, TZ). For further information see Table I. Energies are in kJ/mol.

	SV		**DZ**		**TZ**	
		ΔFCI		ΔFCI		ΔFCI
E_{total}(HF)	-20905.7	–	-20919.7	–	-20926.4	–
E_{corr}(CCSD)	-48.865	0.003	-89.208	0.083	-93.417	0.121
E_{corr}(CCSD(T))	-48.868	0.000	-89.278	0.013	-93.497	0.042
E_{corr}(FCI)	-48.868	0	-89.292	0	-93.538	0
E_{corr}(UCCSD-VQE)	-48.865	0.003	-89.205	0.087	-93.413	0.125
# qubits	10	–	12	–	18	–
# two-qubit gates	1918	–	3096	–	9944	–

Table III. Accuracy of reaction energies for the LiH-dissociation, LiH $\rightarrow$ Li + H, obtained with UCCSD-VQE for basis sets of increasing size (SV, DZ, TZ). The HF, CCSD, CCSD(T), FCI and UCCSD-VQE reaction energies are given together with the respective differences to the FCI reaction energy (ΔFCI). All values are in kJ/mol.

	SV		**DZ**		**TZ**	
		ΔFCI		ΔFCI		ΔFCI
E_{react}(HF)	100.347	-48.691	98.673	-49.399	99.778	-52.443
E_{react}(CCSD)	149.034	-0.003	147.989	-0.083	152.101	-0.120
E_{react}(CCSD(T))	149.038	0.000	148.059	-0.013	152.180	-0.040
E_{react}(FCI)	149.038	0	148.072	0	152.221	0
E_{react}(UCCSD-VQE)	149.035	-0.003	147.985	-0.086	152.096	-0.124

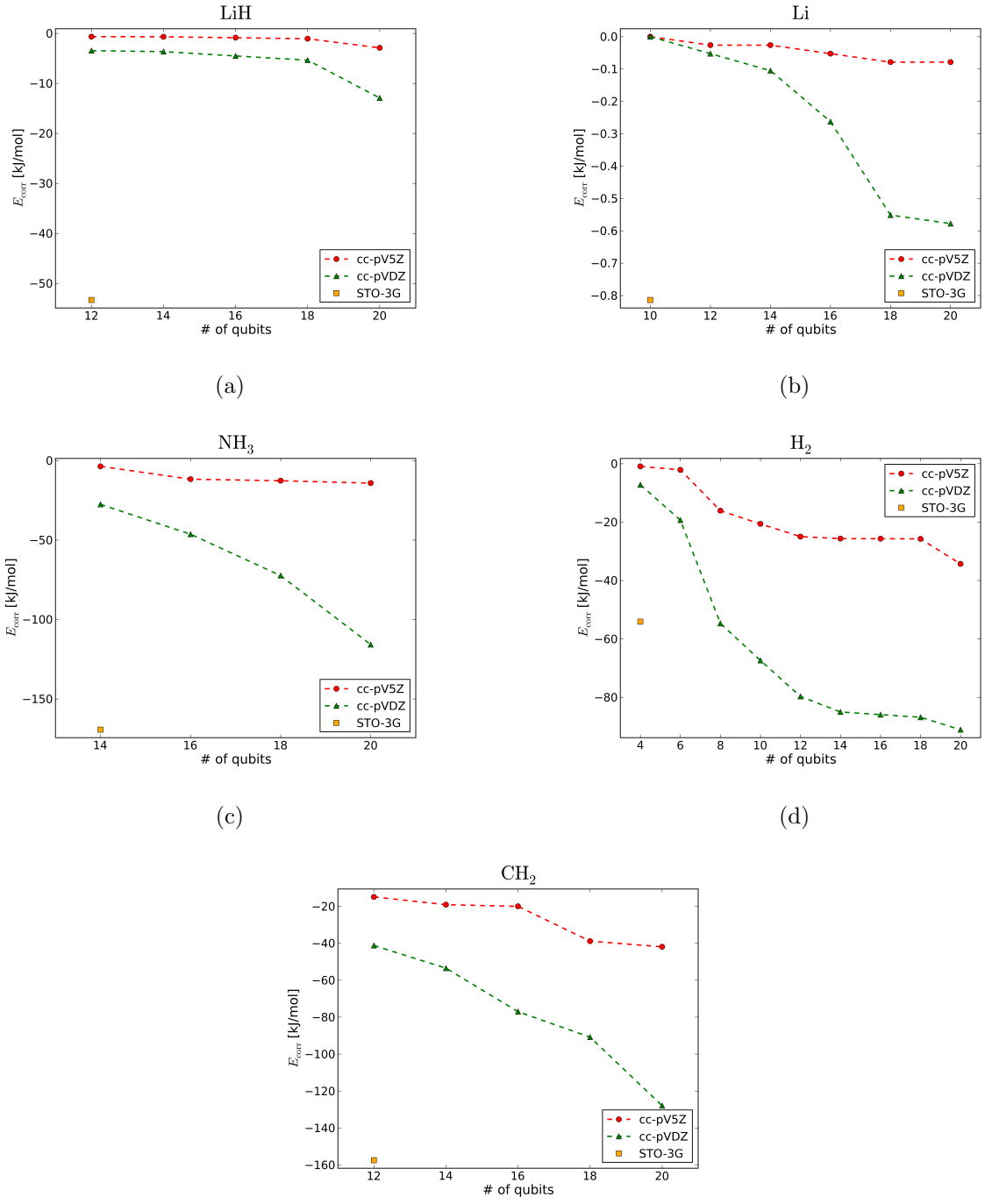

Figure 1. UCCSD-VQE correlation energies for up to 20 simulated qubits. Results are shown for molecules LiH (a), Li (b), NH_3 (c), H_2 (d) and CH_2 (e) in combination with different basis sets (STO-3G, cc-pVDZ and cc-pV5Z).

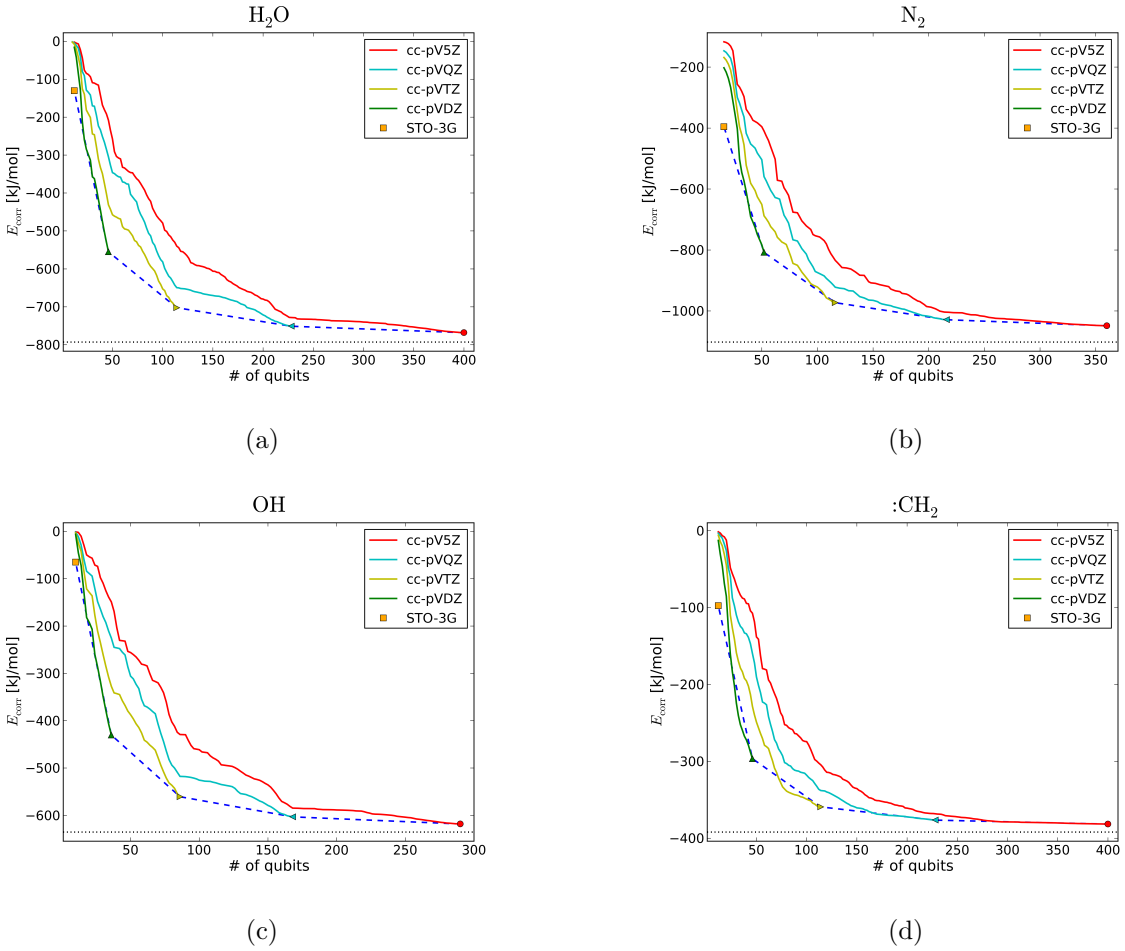

Figure 2. Extrapolated UCCSD-VQE correlation energies for a larger number of qubits. The extrapolation is done by using CCSD correlation energies (worst-case estimates) in accordance with the results shown in Table I in the main paper. Results are depicted for molecules H_2O (a), N_2 (b), OH (c) and $:CH_2$ (d) in combination with basis sets of increasing size (STO-3G, cc-pVDZ, cc-pVTZ, cc-pVQZ and cc-pV5Z). The dotted horizontal line represents the CCSD(T)/cc-pV5Z result which is chosen to be the target/reference energy. For each basis set we gradually increased the number of correlated spin orbitals (= number of qubits) by including more and more of the energetically lowest-lying virtual orbitals. The blue dashed line connects the optimal CCSD correlation energy for each basis set (all virtual orbitals included in the correlation treatment).

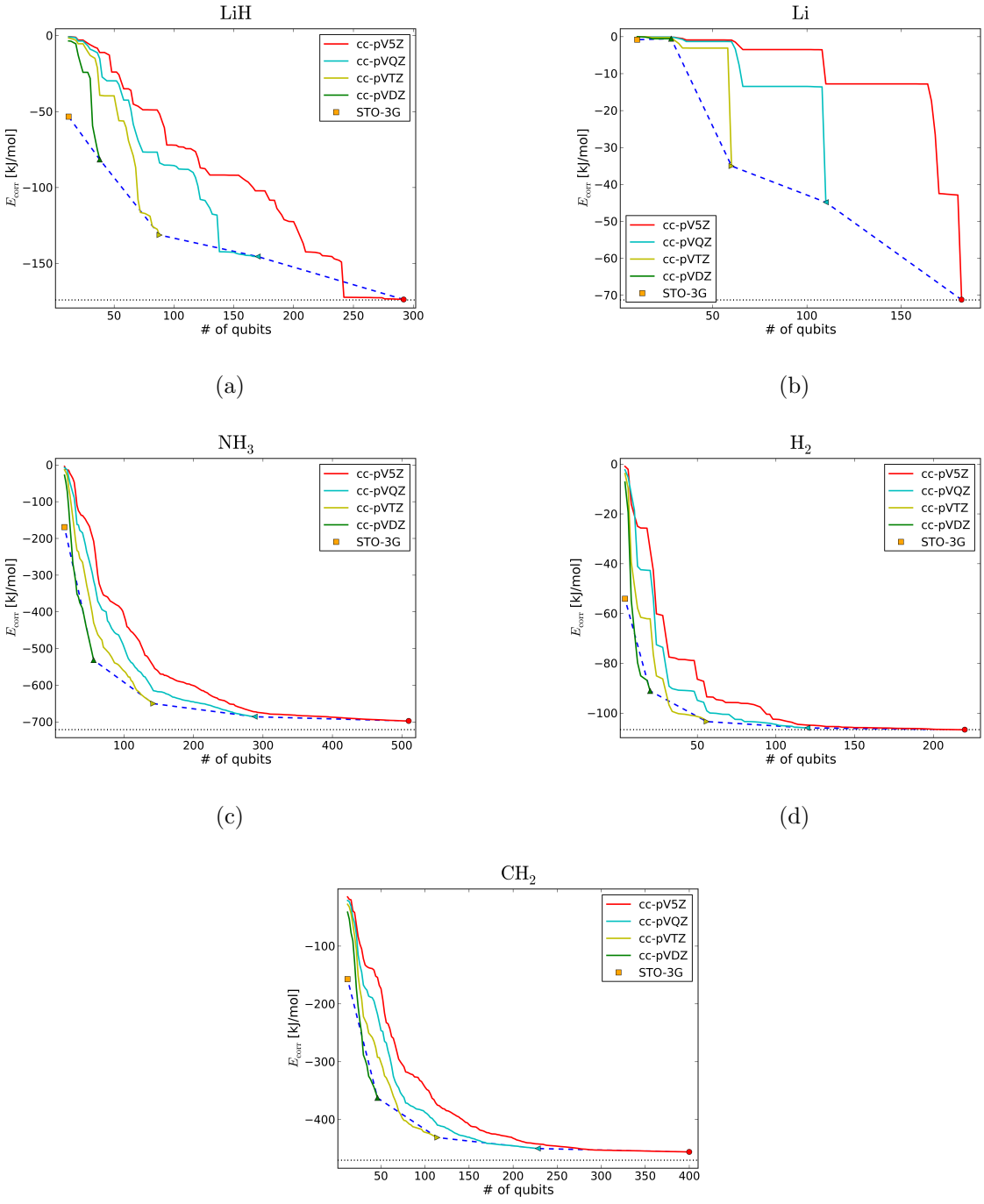

Figure 3. Extrapolated UCCSD-VQE correlation energies for a larger number of qubits. The extrapolation is done by using CCSD correlation energies (worst-case estimates) in accordance with the results shown in Table I. Results are depicted for molecules LiH (a), Li (b), NH_3 (c), H_2 (d) and CH_2 (e) in combination with basis sets of increasing size (STO-3G, cc-pVDZ, cc-pVTZ, cc-pVQZ and cc-pV5Z). For further information see Figure 2.

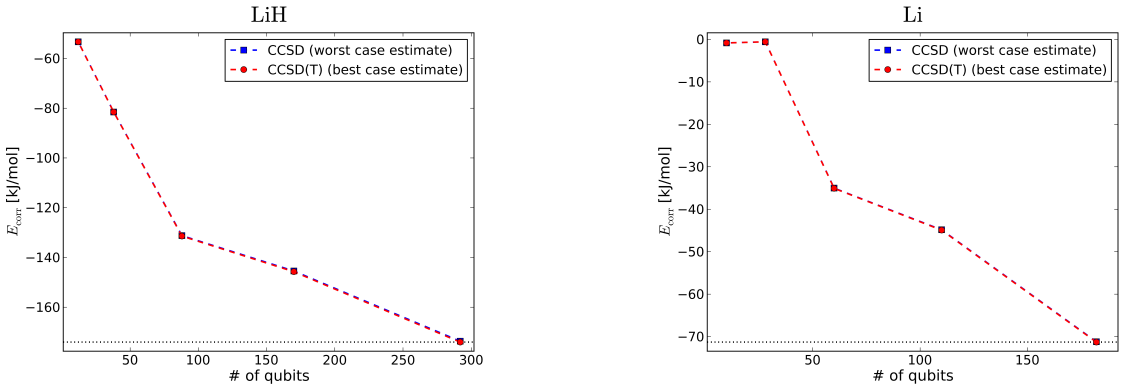

(a)

(b)

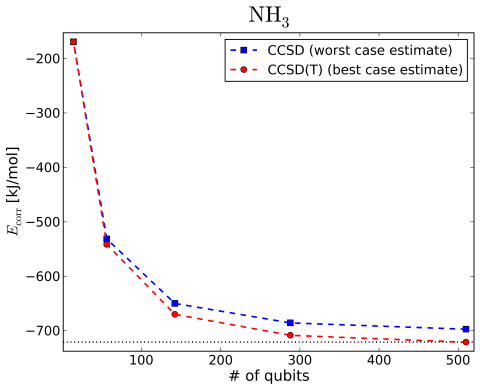

(c)

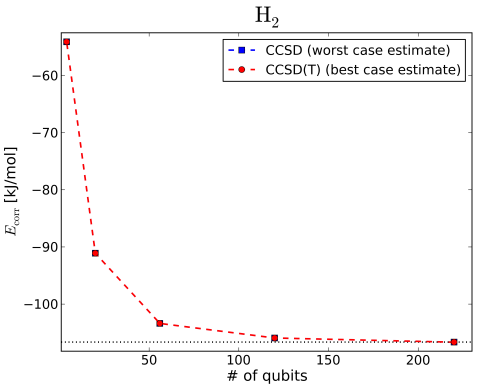

(d)

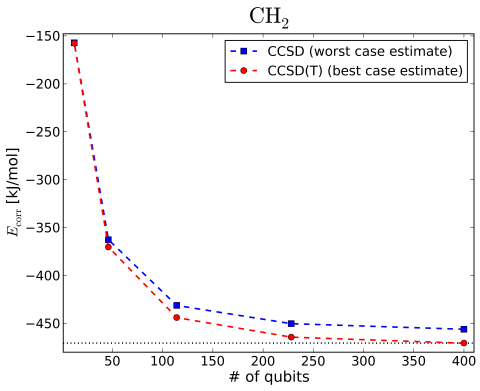

(e)

Figure 4. Extrapolated UCCSD-VQE correlation energies for a larger number of qubits. The extrapolation is done by using CCSD (worst-case estimate) and CCSD(T) (best-case estimate) correlation energies in accordance with the results shown in Table I. For further information see Figure 3.

Table IV. Extrapolated UCCSD-VQE reaction energies for the LiH-dissociation, LiH $\rightarrow$ Li + H, along with corresponding individual molecular energies for basis sets of increasing size (STO-3G, cc-pVDZ, cc-pVTZ, cc-pVQZ and cc-pV5Z). The extrapolation is carried out by using CCSD energies (worst-case estimates) in accordance with the results shown in Table I, as also done in Figures 3 and 4. The obtained CCSD total energies are splitted into a HF total energy contribution and a CCSD correlation energy contribution. For comparison, DFT reaction energies using the functionals BP86, B3LYP and M06-2X are also shown. Additionally, the number of required qubits as well as the number of two-qubit gates are estimated for the computationally most demanding system at a certain basis set quality (here LiH), see also the extrapolation in Figure 9 in the main paper. All energies are in kJ/mol.

		STO-3G	cc-pVDZ	cc-pVTZ	cc-pVQZ	cc-pV5Z
	E_{total}(HF)	-20642.0	-20960.9	-20968.9	-20970.3	-20970.7
LiH	E_{corr}(CCSD)	-53.3	-81.5	-131.2	-145.4	-173.7
	E_{total}(CCSD)	-20695.4	-21042.5	-21100.1	-21115.7	-21144.4
	E_{total}(HF)	-19206.9	-19513.8	-19514.6	-19514.6	-19514.7
Li	E_{corr}(CCSD)	-0.8	-0.6	-35.0	-44.8	-71.2
	E_{total}(CCSD)	-19207.7	-19514.4	-19549.6	-19559.4	-19585.9
H	E_{total}	-1225.0	-1310.9	-1312.3	-1312.6	-1312.7
	$E_{\text{react, total}}$(HF)	210.1	136.2	142.1	143.1	143.3
	$E_{\text{react, corr}}$(CCSD)	52.5	81.0	96.2	100.6	102.5
Reaction	$E_{\text{react, total}}$(CCSD)	262.6	217.2	238.3	243.7	**245.8**
	# qubits	12	38	88	170	292
	# two-qubit gates	$1.5 \cdot 10^3$	$1.7 \cdot 10^4$	$8.3 \cdot 10^4$	$3.0 \cdot 10^5$	$8.5 \cdot 10^5$
	$E_{\text{react, total}}$(BP86)	327.6	237.8	243.3	244.4	244.3
Reaction (DFT)	$E_{\text{react, total}}$(B3LYP)	321.2	238.1	243.6	244.8	244.6
	$E_{\text{react, total}}$(M06-2X)	311.2	230.9	238.4	238.1	237.3

Table V. Extrapolated UCCSD-VQE reaction energies for the Haber-Bosch process, $N_2 + 3\,H_2 \rightarrow 2\,NH_3$, along with corresponding individual molecular energies for basis sets of increasing size (STO-3G, cc-pVDZ, cc-pVTZ, cc-pVQZ and cc-pV5Z). For further information see Table IV. The number of required qubits as well as the number of two-qubit gates are estimated for the computationally most demanding system at a certain basis set quality (here NH_3; in case of STO-3G more qubits are required for N_2 which is the only exception), see also the extrapolation in Figure 10 in the main paper. All energies are in kJ/mol.

		STO-3G	cc-pVDZ	cc-pVTZ	cc-pVQZ	cc-pV5Z
	E_{total}(HF)	-282224.5	-286061.3	-286139.5	-286159.7	-286164.1
N_2	E_{corr}(CCSD)	-395.5	-807.7	-972.7	-1028.6	-1048.4
	E_{total}(CCSD)	-282620.0	-286869.0	-287112.2	-287188.3	-287212.5
	E_{total}(HF)	-2931.8	-2963.4	-2974.6	-2975.9	-2976.3
H_2	E_{corr}(CCSD)	-54.1	-91.1	-103.4	-105.9	-106.7
	E_{total}(CCSD)	-2985.9	-3054.5	-3078.0	-3081.8	-3082.9
	E_{total}(HF)	-145594.2	-147541.4	-147600.0	-147613.7	-147618.0
NH_3	E_{total}	-169.3	-531.5	-650.0	-685.8	-697.4
	E_{total}(CCSD)	-145763.5	-148072.9	-148249.9	-148299.5	-148315.4
	$E_{\text{react, total}}$(HF)	-168.5	-131.1	-136.7	-140.2	-143.2
	$E_{\text{react, corr}}$(CCSD)	219.2	18.0	-17.1	-25.1	-26.4
Reaction	$E_{\text{react, total}}$(CCSD)	50.7	-113.1	-153.9	-165.3	**-169.5**
	# qubits	16	56	142	288	510
	# two-qubit gates	$4.7 \cdot 10^3$	$3.6 \cdot 10^5$	$2.7 \cdot 10^6$	$1.2 \cdot 10^7$	$3.8 \cdot 10^7$
	$E_{\text{react, total}}$(BP86)	-83.6	-145.7	-166.8	-175.0	-180.4
Reaction (DFT)	$E_{\text{react, total}}$(B3LYP)	-108.9	-141.6	-158.6	-167.1	-172.6
	$E_{\text{react, total}}$(M06-2X)	-118.4	-129.0	-156.9	-163.7	-171.7

Table VI. Extrapolated UCCSD-VQE transition energies for the triplet-singlet transition in CH_2, $:CH_2 \rightarrow CH_2$, along with corresponding individual molecular energies for basis sets of increasing size (STO-3G, cc-pVDZ, cc-pVTZ, cc-pVQZ and cc-pV5Z). For further information see Table IV. The number of required qubits as well as the number of two-qubit gates are estimated for $:CH_2$, see also the extrapolation in Figure 11 in the main paper. All energies are in kJ/mol.

		STO-3G	cc-pVDZ	cc-pVTZ	cc-pVQZ	cc-pV5Z
	E_{total}(HF)	-100909.4	-102201.8	-102230.7	-102237.2	-102238.8
:CH$_2$	E_{corr}(CCSD)	-97.6	-296.5	-359.2	-376.4	-381.6
	E_{total}(CCSD)	-101007.0	-102498.3	-102589.9	-102613.6	-102620.4
	E_{total}(HF)	-100745.6	-102082.3	-102111.8	-102119.0	-102121.0
CH$_2$	E_{corr}(CCSD)	-157.2	-362.6	-431.2	-450.2	-456.0
	E_{total}(CCSD)	-100902.8	-102444.9	-102543.0	-102569.2	-102577.0
	$E_{\text{react, total}}$(HF)	163.7	119.5	118.9	118.1	117.8
	$E_{\text{react, corr}}$(CCSD)	-59.6	-66.2	-72.0	-73.8	-74.4
Reaction	$E_{\text{react, total}}$(CCSD)	104.1	53.4	46.9	44.3	**43.4**
	# qubits	12	46	114	228	400
	# two-qubit gates	$1.8 \cdot 10^3$	$6.9 \cdot 10^4$	$5.0 \cdot 10^5$	$2.1 \cdot 10^6$	$6.6 \cdot 10^6$
	$E_{\text{react, total}}$(BP86)	94.3	68.9	66.7	65.9	65.4
Reaction (DFT)	$E_{\text{react, total}}$(B3LYP)	80.2	52.8	50.2	49.2	48.7
	$E_{\text{react, total}}$(M06-2X)	88.6	58.8	56.5	55.8	56.6

Table VII. Coordinates of H_2O obtained at the B3LYP/def2-QZVPP level.

O	0.0044960	0.0057136	0.0000000
H	0.9646713	-0.0073990	0.0000000
H	-0.2330023	0.9361335	0.0000000

Table VIII. Coordinates of OH obtained at the B3LYP/def2-QZVPP level.

O	-0.0062713	0.0000000	0.0000000
H	0.9674223	0.0000000	0.0000000

Table IX. Coordinates of LiH obtained at the B3LYP/def2-QZVPP level.

Li	-3.2319355	1.1691641	0.0000000
H	-1.6405907	1.1691641	0.0000000

Table X. Coordinates of N_2 obtained at the B3LYP/def2-QZVPP level.

N	-4.2451484	2.5760816	0.0000000
N	-3.1862016	2.3168784	0.0000000

Table XI. Coordinates of H_2 obtained at the B3LYP/def2-QZVPP level.

H	-4.0759023	2.5346545	0.0000000
H	-3.3554477	2.3583055	0.0000000

Table XII. Coordinates of NH_3 obtained at the B3LYP/def2-QZVPP level.

N	-0.6800848	1.2693644	0.0227335
H	0.3314114	1.2772854	-0.0142918
H	-0.9994515	0.5770216	-0.6429998
H	-0.9993852	2.1717686	-0.3063819

Table XIII. Coordinates of $:CH_2$ obtained at the B3LYP/def2-QZVPP level.

C	-2.8332513	0.6986016	0.0000000
H	-1.8294369	1.0885324	0.0000000
H	-3.8206119	1.1284960	0.0000000

Table XIV. Coordinates of CH_2 obtained at the B3LYP/def2-QZVPP level.

C	-2.8371013	0.5067306	0.0000000
H	-1.9616221	1.1871592	0.0000000
H	-3.6845767	1.2217402	0.0000000